Experimental Investigation of the Interaction Radiation of a Moving Electron with a Metallic Grating: The Smith-Purcell Effect

J. P. Bachheimer*
Laboratoire de Spectrométrie Physique associé au Centre National de la Recherche Scientifique Cedex 53, 38-Grenoble-Gare, France
(Received 6 December 1971)

In order to test a previously proposed theory of the Smith-Purcell effect, experimental results for the linewidth, the radiation patterns, and the absolute emitted power from aluminium and silver gratings are reported. The measurements are made at 130 kV in the ultraviolet and visible range with gratings of 1221.2 lines/mm. For this purpose, we recall the theoretical formulas for the power and the line breadth as a function of the incidence angle of the electrons on the grating: These two quantities characterize the emission mechanism. We then show briefly how various experimental parameters can affect the results. We thus deduce that the observed radiation does indeed arise from the process initially proposed (i.e., diffraction of the electron field). The line breadth agrees well with the theory. With the assumption that the average groove profile is close to that claimed by the manufacturer (in fact the grooves appear irregular in electron-microscope measurements) the theory accounts for the main features of the observed dependence of the power and radiation patterns upon the wavelength and the metal. Numerical calculations of the influence of the profile show that within the experimental error the theory satisfactorily predicts the absolute emitted power. A rise in intensity is measured at the surface plasma wavelength for Ag; this is in agreement with the theory.

I. INTRODUCTION

Smith and Purcell[1] first demonstrated, that an electron passing close to an optical diffraction grating and perpendicular to the grating rulings can produce visible polarized light. They explained this effect in terms of the radiation from induced surface charges which are periodically accelerated. Smith[2] verified that the wavelength λ is given by the formula

$$\lambda = (d/n)\,(1/\beta - \sin\theta_n)\,, \quad n = 1, 2, 3, \ldots \tag{1}$$

where d is the grating-ruling spacing, β is the ratio of the electron velocity to the velocity of light, and θ_n is the angle between the direction of emission and the normal to the trajectory of the electron. Further, he showed by an approximate theory that the emission intensity must decrease exponentially as the distance between the electron and the grating increases. Other experiments[3-5] have since been reported but no quantitative results with well-defined conditions were given. Recently, Salisbury[6] (who patented a device based on a similar principle in 1949) has concluded from his later experiments that the proposed emission mechanism is unsatisfactory. Bachheimer and Bret have pointed out[7] the ambiguity of the radiation process because the electrons must strike the grating to obtain detectable emission. However, it has been shown[8] by study of the influence of the angle of incidence of the electrons on the grating that near grazing incidence the radiation from the induced current is measurable.

The purpose of this article is to compare experimental measurements of the absolute intensity and width of the emitted line with a theory which we have previously proposed.[9] The measurements were made in the visible and ultraviolet region and were obtained from Al and Ag gratings. In particular, there appeared, near the surface-plasmon frequencies, a rise in intensity due to radiative transformation of plasma surface waves. In order to analyze the results, it is necessary to discuss the influence of certain experimental parameters. This is done in Sec. III after a summary, in Sec. II, of the main theoretical results. The apparatus is briefly described in Sec. IV, and the experimental results are discussed in Sec. V. Section VI summarizes the conclusions.

II. SUMMARY OF THE THEORY

The calculation of the Smith-Purcell effect was performed[9] (from a classical viewpoint) by reducing the problem to the diffraction of the evanescent waves associated with the moving electron, following Toraldo di Francia.[10] Each electron, in the absence of interaction with its neighbors, moves with an initial trajectory parallel to the median plane of the grating lines. The metal is described by its dielectric constant $\epsilon(\omega) = (\nu + i\chi)^2$ (ν index of refraction, χ extinction coefficient). The incidence plane is defined, as usual, by the normal to the grating plane and the electron trajectory. In this plane, when the electron beam is thick [i.e., $\gg \lambda/4\pi\xi$; $\xi = (1-\beta^2)^{1/2}/\beta$] and grazes the top of the grooves, the following numerical expression has been obtained for the power in the nth order:

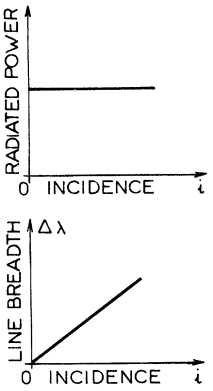

FIG. 1. Simultaneous theoretical variations with the incidence angle of the line breadth and the radiated power from electrons passing over the grating.

$$dP_n(\mathrm{W}) = 7.2\times10^{-8}\,|I|\left(\frac{\mathrm{A}}{\mathrm{cm}^2}\right)\frac{S(\mathrm{cm}^2)}{d(\mathrm{cm})}\,\frac{l}{R}\,\frac{d\lambda}{\lambda}\,p_n\,, \tag{2}$$

where I is the current density of the electron beam, S is the source area (as seen by the optical detection system), l is the width of detector, R is the distance from the detector to the origin, and $p_n = (1/\xi)(d/\lambda)\cos\theta_n |b_n(\nu, \chi, \lambda)|^2$ is the "power factor." $b_n(\nu, \chi, \lambda)$ represents the amplitude of the diffracted field, above the grooves, excited by the electron. The calculation of b_n constitutes the electromagnetic diffraction problem which we wish to solve. In the Rayleigh-expansion approximation which we used, we showed that the b_n are solutions of an infinite system of equations which is solved by taking increasingly large truncated systems until the b_n converge.[11] The convergence of the process depends on the groove shape and, in general, is good for shallow grooves. A numerical test is necessary in each case.

Further, we considered the case of a trajectory with a small angle of incidence i with the grating plane (this case is in fact a better approximation to the experimental situation as it is practically impossible to obtain a rigorous parallelism between the grating and the electron beam which has always some divergence itself). We found that the total energy radiated by an electron varies as $1/\sin i$.[12] Consequently, the power radiated by a perfectly parallel electron beam is also given by (2). Because the exponential variation of the intensity ($\sim e^{-4\pi t h/\lambda}$) with the height h of the electron above the grating, the emitted wave train is exponential and thus exhibits a Lorentzian line shape with half-width given by

$$\Delta\lambda = 2\xi\frac{d}{n}\sin i = \frac{\Delta\lambda_0}{1-\beta\sin\theta_n}\,, \quad \Delta\lambda_0 = 2\beta\xi\lambda\sin i\,. \tag{3}$$

Thus, for a source with constant surface area, the mechanism of emission by radiation from the diffracted field of the electron is characterized by simultaneous variations of the power and the line breadth as shown in Fig. 1.

III. INFLUENCE OF SOME EXPERIMENTAL PARAMETERS

When the angle of incidence increases, the above relations may be altered for the special case of the echelette grating in the optical range,

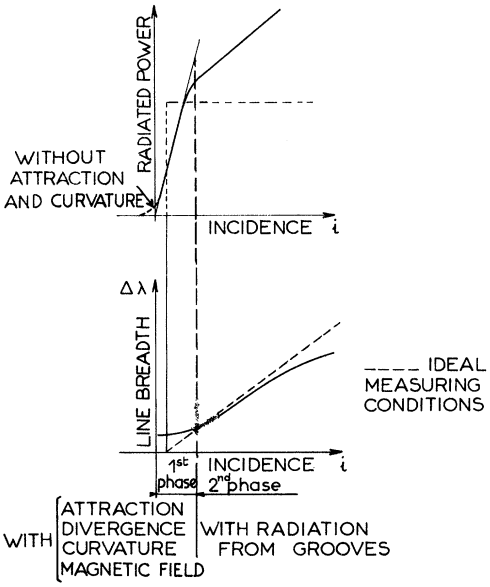

FIG. 2. Radiated power and line breadth (general theoretical shapes, taking into account several experimental conditions).

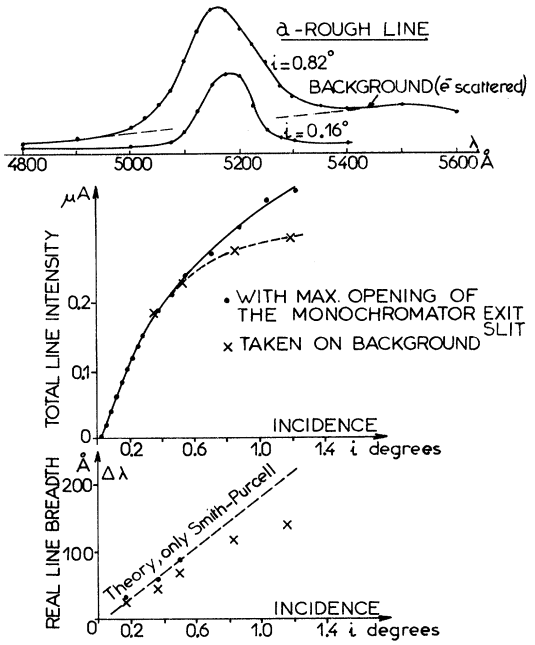

FIG. 3. Ag grating with 1221.2 lines/mm, blaze 5°15′. Measured power and line breadth as a function of incidence angle at 130 kV for $\lambda = 5200$ Å; $n = 2$.

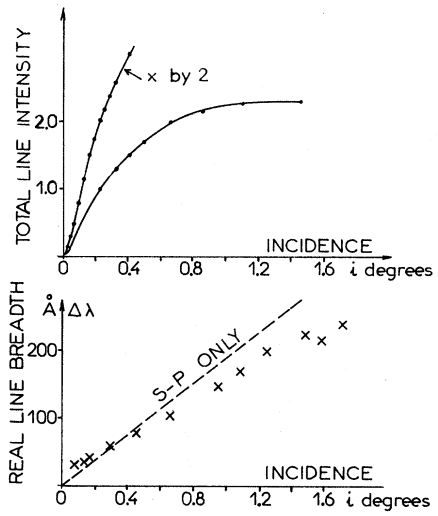

FIG. 4. Ag grating with 1221.2 lines/mm, blaze 5°15′. Measured power and line breadth as a function of incidence angle at 130 kV for $\lambda = 4500$ Å; $n = 2$.

since the electron striking the grating has a non-negligible probability of crossing several grooves.[13] Consequently, the emitted wave train is prolonged (during the passage through the grooves the transition radiation, a process which is not fundamentally different from the Smith-Purcell effect, is generated). The line breadth therefore decreases, while the total energy increases. The importance of these modifications obviously depends on the scattering properties of the metal and on the relative energy radiated when the electron is above the grooves and when it is in the grooves. If one assumes that the average path is independent of the incidence angle and that the average energy radiated in the groove is equal to the average energy radiated above it, it can be shown by a semiquantitative calculation[14] that the effect on the line breadth is smaller than the effect on the power. For instance, with a 3-groove path in a 600-lines/mm grating with 130 kV ($\beta = 0.6$) electrons and at $\lambda = 0.5$ μm the power increases by a factor of 2 over 0.35° but the line breadth decreases only by 2%. When the incidence angle decreases, the emitted radiation above the groove (the Smith-Purcell effect) becomes dominant, and we can verify[8] that the line breadth is independent of the metal. However, other physical parameters enter which cause the line breadth to increase and the power to decrease. Quantitative arguments are given in Ref. 14. Here, we describe briefly their effect.

The electrostatic attraction of the electron by the grating bends the trajectory and thus limits the wave train. This effect is shown to depend strongly on the electron-grating distance. Consequently, the electron density in the surface source decreases. This decrease becomes negligible beyond a certain value of the angle of incidence. Thus the line breadth possesses a lower limit; The residual magnetic field also bends the trajectory thus adding to the lower limit.

Both effects increase rapidly as the electron velocity decreases. For example if we suppose an infinitely conducting plane in place of the grating, we find, at 130 kV, $\lambda = 0.5$ μm, a line breadth corresponding to 0.06° for the attraction and field effects ($B = 0.5$ G assuming the source is 15-mm distant from the grating edge); this quantity increases to 0.26° for the attraction and 0.11° for the field effect at 10 kV.

Other effects which increase the line breadth or decrease the power are: A slightly curved substrate can reduce the power (the $1/\sin i$ behavior is no longer valid); The divergence of the electron

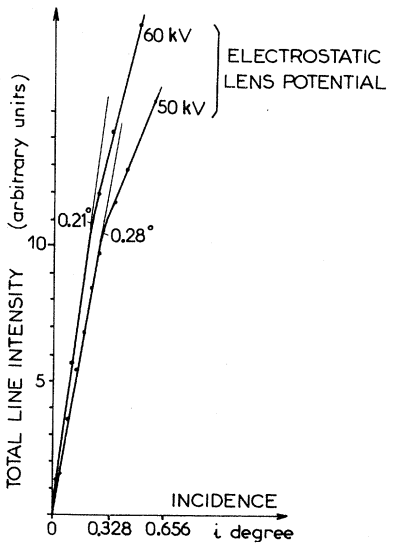

FIG. 5. Ag grating with 1221.2 lines/mm, blaze 5°15′. Measured power as a function of incidence angle, influence of the electron beam divergence at 130 kV ($\lambda = 0.45$ μm; $n = 2$).

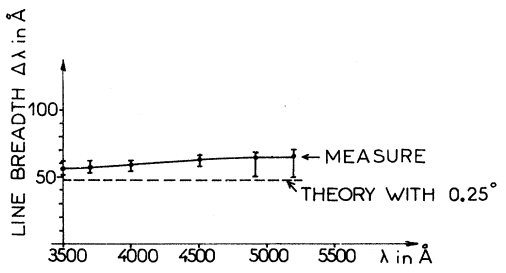

FIG. 6. Ag grating with 1221.2 lines/mm, blaze 5°15′. Line breadth versus λ for n constant at 130 kV ($i \simeq 0.25°$; $n = 2$).

beam generally produces electrons with various incidence angles in a given surface element. Each angular segment radiates with an angular displacement relative to the next; the power is consequently reduced. This effect vanishes progressively as the average primary incidence angle becomes larger than the divergence of the beam.

Finally, the dependence of the power and the line breadth on the incidence angle must take the general form shown in Fig. 2, rather than that shown in Fig. 1. Furthermore, numerical tests[14] show that the radiation corresponding to the emission of a perfect parallel beam can be taken at the break in the slope if neither the divergence nor the participation of radiation from the grooves is high (sometimes the break is imperceptible).

IV. APPARATUS

The essentials of the apparatus have been published elsewhere.[7] An evaporation device[13] and a system for measuring the electron density[14] in the surface source have been added. We shall briefly describe the main characteristics of the device. A high-stability generator [Societé Anonyme de Machines Electrostatiques, Grenoble (S. A. M. E. S.)] accelerates the electrons up to a maximum of 140 kV. The rapid fluctuations are only ±15 V, so that the effect on the line breadth is negligible. The rectangular (25×0.5 mm) electron beam, collimated by an electrostatic lens (divergence ~0.15°), passes close to a movable tungsten knife then in front of the grating which is mounted on a micrometric ball knee and can also be moved in a direction perpendicular to the beam. The beam is collected in a very deep collector connected to the ground through an ammeter. The grating is a master engraved on Al evaporated on to a hollow metal blank to facilitate cooling. An oil-free vacuum is obtained using Varian zeolith and ion pumps; as an additional precaution the grating is maintained at 100 °C. The radiation is collected in the incidence plane by a movable spherical mirror which determines the angle θ_n. The radiation is then sent to the entrance slit of a Hilger-Watt D 323 monochromator by means of a catadioptric system. The monochromator is preceded by a linear polarizer (Polaroid sheet) and followed by a photomultiplier. The absolute spectral sensitivity of the optical detection system is obtained from a standard tungsten-ribbon lamp using Devos's emissivity.[15] Electrostatic deviation plates make it possible to modulate the emission. The quartz-controlled, vacuum-evaporation system allows one to deposit on half of the grating a silver coating of 3200 Å thickness maximum. The beam current density is obtained from the variation in the collector current produced by the displacement of a tungsten diaphragm placed just before the grating. At the position where the Smith-Purcell intensity is halved, the slope of the curve of current versus the diaphragm displacement gives directly the average current density in the source area.

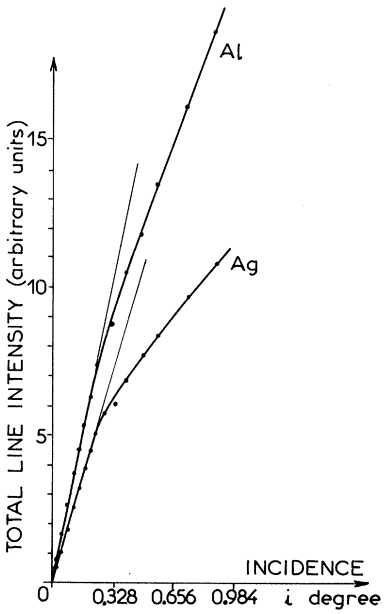

FIG. 7. Al and Ag grating with 1221.2 lines/mm, blaze 5°15′. Search for the correct incidence angle to compare measured absolute emitted power with theory.

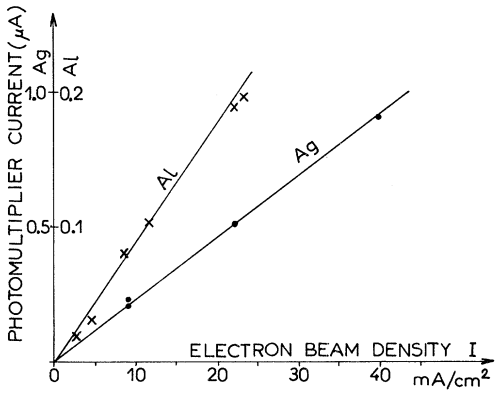

FIG. 8. Linearity of the Smith-Purcell intensity with the electron beam density (1221.2 lines/mm, 5°15′, Al and Ag, 130kV, $\lambda = 4920$ Å; $n = 2 - i \simeq 0.26°$).

V. EXPERIMENTAL RESULTS

A. Procedure

The radiation pattern is obtained by rotating the collector mirror and recording the signal from the exit slit of the monochromator. The entrance slit determines the receiving solid angle (corresponding to $\Delta\lambda$ of a few angstroms). The total energy

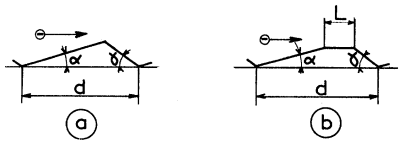

FIG. 9. Definition of the profiles used in calculation.

from a line is found by widening the exit slit until no further increase in the signal occurs. It is sometimes necessary, particularly when there is a large continuous background (due to the electrons scattered in the grooves) to sweep the line against λ. This is generally the case for large incidence angles. The area under the curve obtained in this way is proportional to the energy of the emitted line. From this curve the real slope of the line is obtained using a deconvolution calculation[13] as it is known that the line is Lorentzian. This last fact was carefully checked using a negligible background.[14]

B. Results

We have already reported[7] that the line breadth shows a Doppler broadening (largest in the forward direction) and is independent of the metal[8] for small incidence angles, in agreement with the theory, in spite of the deep grooves used in the experiment.

The following results concern an echelette grating with 1221.2 lines/mm and a 5° 15′ blaze. This can still be considered as shallow and so gives good convergence in the Rayleigh approximation.

The observations were made in the 3300- to 5780-Å range using a E. M. I. 6256 B photomultiplier. The source area is a few square millimeters while the solid angle is about 10^{-4} sr. The polarization is nearly 100% in the incidence plane.

Figures 3 and 4 show two examples of the dependence of total power and line breadth upon the incidence angle (the dashed curves are the line breadths arising from radiation over the grooves). The general behavior closely resembles that of Fig. 2 if it is supposed that the participation of scattered electrons causes a change of the slope after the divergent-beam region. The line breadth is not always easy to estimate [see Fig. 3(a)] as the background is sometimes large, especially at large incidence angles. However, at large incidence angles the line breadth is smaller than predicted by theory, whereas it becomes progressively larger as the incidence angle decreases. According to Fig. 2 this effect takes place approximately at the break. Figure 5 illustrates the influence of the beam divergence on the intensity. If we sum the effects of the beam divergence (0.15°), the theoretically estimated electrostatic attraction (0.03°) and the magnetic field (0.03°) we obtain a value of 0.21° which agrees well with the measurements. Figure 6 shows that, in the neighborhood of the break, the line breadth is indeed caused by the radiation coming from above grooves according to formula (3), i.e., independent of λ for constant n. Thus comparing the calculations with the measured variations of the line breadth and the intensity with incidence angle, we can assert that the radiation indeed arises from the interaction above the grooves in accordance to the mechanism considered in the theory. We can now compare the experimentally observed patterns and absolute power with the calculations. According to Sec. II, we look for the break in the increase in intensity to determine the incidence

FIG. 10. Specimens of the profile of the 1221.2 lines/mm, blaze 5°15′, grating used in our experiments. (1) silver; (2) aluminum (incompletely engraved zone) (from Laboratoire d'Optique et de Physique Cristalline de la Faculté des Sciences de Marseille, France).

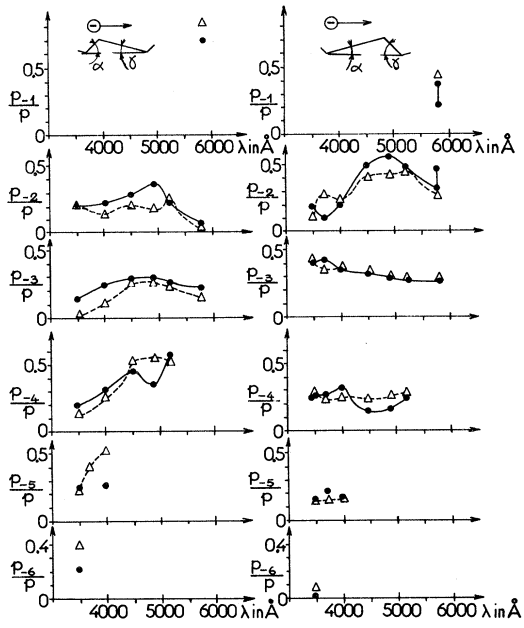

FIG. 11. Experimental and theoretical radiation patterns from a 1221.2-lines/mm Al grating at 130 kV as a function of λ. Solid line ● : experimental points; dotted line △: theoretical points with $\alpha = 35°$, $\gamma = 5°15'$; $\alpha = 5°15'$, $\gamma = 35°$.

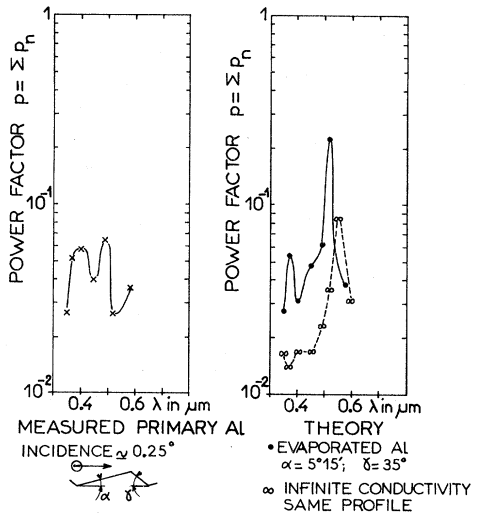

FIG. 12. Comparison of the measured and calculated absolute power at 130 kV from Al grating (1221.2 lines/mm; 5°15′).

angle which gives only Smith-Purcell radiation. From Fig. 7 we find, for both Al and Ag, $i \sim 0.25°$. We have carefully checked the linear dependence upon S, l, $d\lambda$ in formula (2). Figure 8 shows that the emitted power is related linearly to the beam current density in the source area (this is simultaneously a test of the measuring device).

We shall describe the emitted power in terms of the "power factor" $p = \sum p_n$ from which we can then calculate the power for any I, S, l, R, $d\lambda$. The relative pattern is characterized by p_n/p. These values are obtained from (2) in a straightforward manner.

The estimated accuracy of the measurements are approximately

$$\Delta p/p = \pm 25\%, \quad \Delta p_n/p_n = \pm 10\%.$$

To be able to compare with the theory, it is necessary to know the true profile of the grooves. This can be very different from the ideal [Fig. 9(a)] profile described in the manufacturer's catalog, defined by $\alpha = 5° 15'$; $\gamma = \frac{1}{2}\pi - 5° 15'$. Using the procedure described in Ref. 16, an electron-microscope examination showed that our grating is irregularly and often incompletely engraved: It is practically impossible to define the angles α and γ (Fig. 10). In spite of this surprising observation it appears that the main characteristic results can be explained on the assumption that the average profile is not much different from that claimed by the manufacturer. Thus, we first use this average profile as a basis for our comments on experiments. We shall discuss later the influence of the profile variations.

C. Results on Primary Al

At 130 kV, the radiation pattern as a function of λ and the orientation of the grooves are shown in Fig. 11. The calculations are performed with $\alpha = 5° 15'$, $\gamma = 35°$ [Fig. 9(a)], and the orientation (not determined experimentally) is adjusted to give the best fit. The values of ν and χ are taken from Ref. 17. The similarity between the theoretical and experimental curves is striking: The dependence of the experimental patterns on the groove orientation agrees well with the theory. In Fig. 12 the dependence of the "power factor" is shown as a function of λ. Experimentally two small maxima of radiation occur at about 4920 and 4000 Å; with evaporated Al the calculation predicts sharp maxima at 5200 and 3700 Å. This discrepancy could be attributed to the uncertainty in our knowledge of ν and χ, the indices of the original aluminum which may be considerably different from the published values, due to surface conditions (such as oxide coat, asperities, etc.). Further, it is possible that the detailed profile of the grooves has a non-negligible influence. We also notice that the experimental points overlap the theoretical curve,

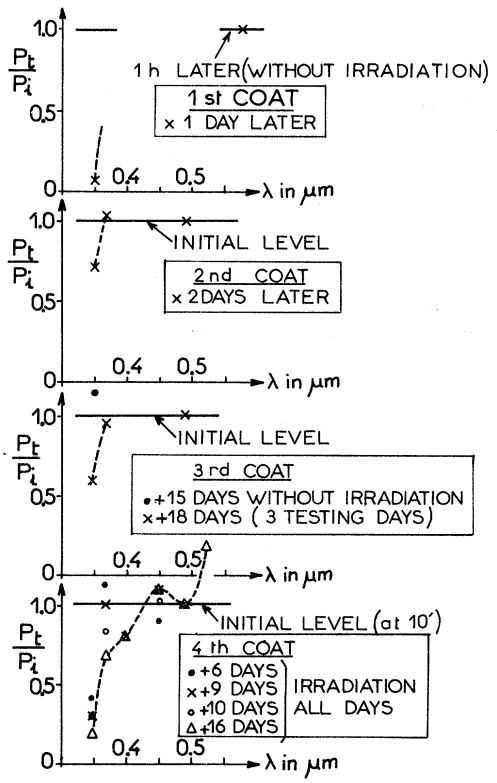

FIG. 13. Decrease of the measured power as a function of time after the evaporation. The intensity of the line 4920 Å, $n = 2$ is taken as reference level except for the first coat where we have taken the 5780 Å, $n = 2$ line.

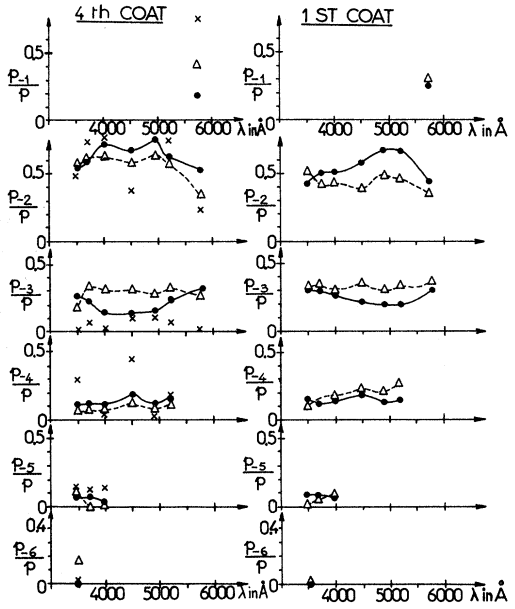

FIG. 14. Experimental and theoretical radiation patterns from a 1221.2-lines/mm Ag grating at 130 kV as a function of λ. Results from first and fourth coat. Note: If we assume $\gamma = 11°$ instead of $\gamma = 22°$, we see that the theory is incompatible with the experiment. Solid line, •: experimental points; dotted line, △: theoretical points with first $\alpha = 5°15'$, $\gamma = 35°$; fourth $\alpha = 5°15'$, $\gamma = 35°$ ($\times\gamma = 11°$).

the extreme points practically coinciding (although this is perhaps fortuitous because the accuracy of the measurements is not high).

D. Results on Ag at 130-kV Radiation from Surface Plasmons

Special attention was paid to the wavelength $\lambda = 0.35\ \mu m$ at which the radiation of plasma surface waves is theoretically predicted. On top of the Al primary four coats of Ag were evaporated (1 = + 850, 2 = + 550, 3 = + 300, 4 = + 1500 Å). In each case, the intensity of the line $\lambda = 3500$ Å decreased with time, taking as reference the $\lambda = 4920$ Å, $n = 2$ line (Fig. 13). For instance, we note for the fourth coat that over a period of 16 days the intensity diminished to 20% of its initial value, while for $\lambda = 4920$ Å the intensity remained constant (to within 10%). For the first coat the intensity at 5780 Å was constant (initial reference) but the intensity at 3500 Å was observed to have fallen to 90% 1 day later. The critical period seems to be during the bombardment, but this is not certain as no systematic measurements were made. For all coats, at 3500 Å, while the intensity decreased, the relative pattern of radiation remained the same. At this value of λ, such attenuation is a sign of radiation from surface plasmons, which are very sensitive to contamination.[18] The origin of this contamination has not been determined, but it is certainly not due to residual oil vapor, there being no detectable deposit observed after dismantling. It is possible that the vacuum ($\sim 10^{-6}$ Torr) is not sufficiently good. In Fig. 14 the evolution of the radiation patterns is shown for the first and the fourth coat. For the latter, we note that the second order radiates appreciably more than the first. Such an increase is found theoretically (ν, χ taken from Ref. 19) if it is supposed that the profile is attenuated by the coat ($\gamma = 22°$ instead of $\gamma = 35°$). Figure 15 shows the experimental and theoretical change of pattern as a function of the metal; the agreement is very good. Figure 16 shows the total power for the fourth coat whose thickness 1500 Å is greater than

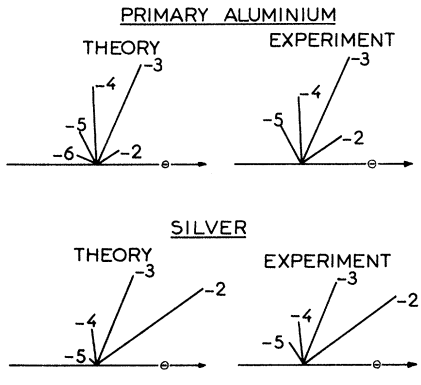

FIG. 15. Experimental and theoretical radiation patterns from 1221.2 lines/mm Ag grating at $\lambda = 3500$ Å, first coat, 130 kV. Theory with $\alpha = 5°15'$ $\gamma = 35°$. (The lengths of the intensity bows are proportional to p_n/p.)

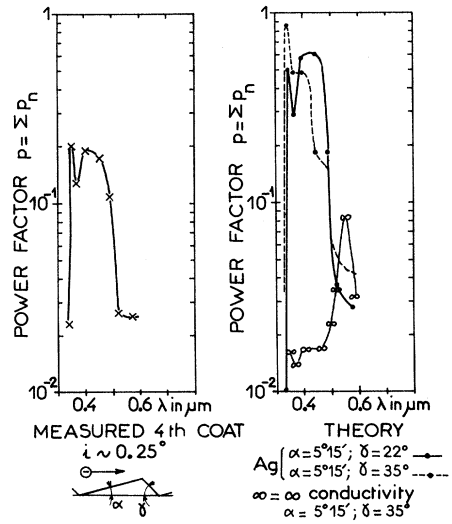

FIG. 16. Comparison of the measured and calculated absolute power at 130 kV from Ag grating (1221.2 lines/mm, 5°15').

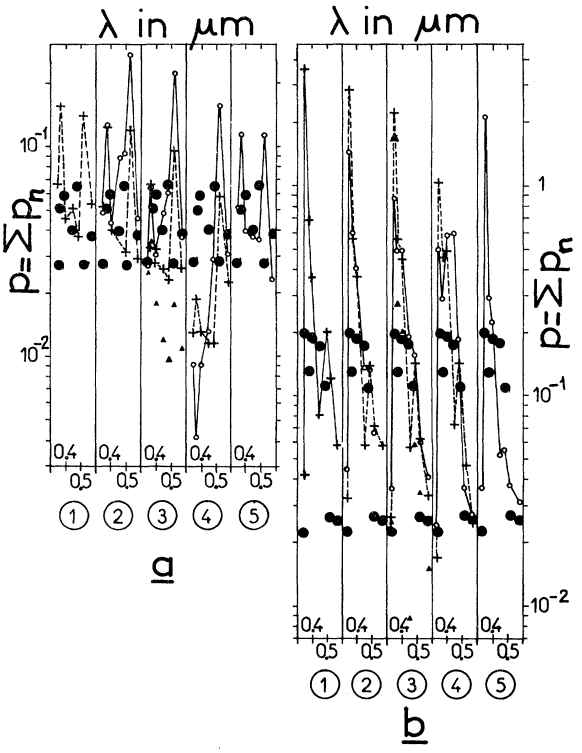

FIG. 17. Influence of the shape of the profile on calculated (+, ○, ▲) (1221.2 lines/mm, 130 kV) power (● experiment). (a) aluminum: 1: $\alpha=8°, \gamma=45°$, + $L/d=0.5$; 2: $\alpha=5°15'$, $\gamma=45°$, ○ $L/d=0$, +$L/d=0.4$; 3: $\alpha=5°15'$, $\gamma=35°$, ○ $L/d=0.0$, +$L/d=0.4$, ▲ $L/d=0.6$; 4: $\alpha=5°15'$, $\gamma=22°$, ○ $L/d=0$, +$L/d=0.4$; 5: $\alpha=3°$, $\gamma=45°$, ○ $L/d=0.0$. (b) silver: 1: $\alpha=8°$, $\gamma=45°$, + $L/d=0.5$; 2: $\alpha=5°15'$, $\gamma=45°$, ○ $L/d=0$, + $L/d=0.4$; 3: $\alpha=5°15'$, $\gamma=35°$, ○ $L/d=0$, + $L/d=0.4$, ▲ $L/d=0.6$; 4: $\alpha=5°15'$, $\gamma=22°$, ○ $L/d=0$, + $L/d=0.4$; 5: $\alpha=3°$, $\gamma=45°$, ○ $L/d=0$.

that of the previous three. We arranged the setup to make a rapid measurement at 3500 Å. With $\gamma=22°$ the theory reproduces the experimental variations if a reduction factor is included. In particular it shows the peak at 3500 Å and the radiation cutoff at the shortest wavelengths (connected with the bad reflectance in this range). As for Al, the experimental and theoretical powers at 5780 Å are in close agreement. The reduction factor reaches 3 at 4500 Å but is only 1.8 at 4920 Å. In this range of wavelengths there are many possible causes to explain this factor.

The tests were made 10 min after the evaporation. During this time contamination of the coating may take place, particularly as the grating is at 100 °C. Theoretically we consider infinitely thick silver; experimentally we have many coats on an irregular profile in Al. The boundary conditions are not exactly the same for the surface-plasma oscillations which could give just such a damping near the surface-plasma wavelength. The real microprofile is different from the average profile taken in the calculation. To see how the profile influences the radiation patterns and the absolute emitted power we have taken different cases [Figs. 9(a) and 9(b)] giving good convergence for calculation for a depth between 400 and 700 Å (for perfect engraving, the depth would be 760 Å). We shall discuss separately the influence on power and on the patterns. (a) Influence of the slope of the grooves on the emitted power: Figure 17 gives some examples. In these a top flattened by $L/d=20\%$ [Fig. 9(b)] has no appreciable influence on the results; thus a $L/d=40\%$ flattened top has been given as an example in some cases. For Al, the two maxima at 5200 and 3700 Å are everywhere observed except at one point (these two maxima vanish at 105 kV, i.e., $\beta=0.55$). Further, the experimental points are grouped in the region of theoretical points. This shows that the emitted power does not change very much with the details of the profile. We note however certain limits: With grooves that are too shallow ($\alpha=5°\ 15'$,

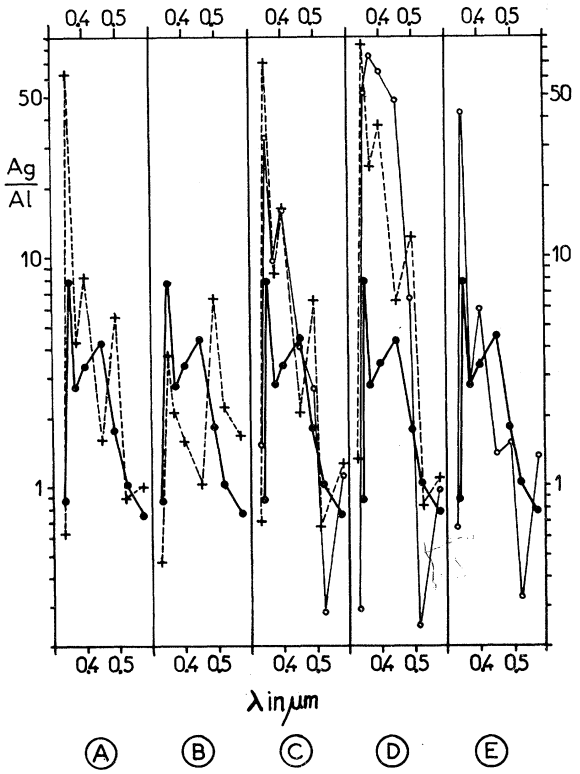

FIG. 18. Calculated (○,+) (1221.2 lines/mm, 130 kV) ratio of the power radiated by Ag to the power radiated by Al as a function of λ for various profiles (● experiment): A: $\alpha=8°$, $\gamma=45°$, $+L/d=0.5$; B: $\alpha=45°$, $\gamma=8°$, $+L/d=0.5$; C: $\alpha=5°15'$, $\gamma=35°$, ○ $L/d=0$, $+L/d=0.4$; D: $\alpha=5°15'$, $\gamma=22°$, ○ $L/d=0$, $+L/d=0.4$; E: $\alpha=3°$, $\gamma=45°$, ○ $L/d=0$.

TABLE I. Calculated variations of the radiation patterns with the orientation of grooves for various profiles (Al, $\lambda = 5780$ Å, 1221.1 lines/mm, 130 kV). Comparison with the experiment.

	p_n/p calculated							
	$L/d = 0.0$		$L/d = 0.4$		$L/d = 0.5$		Experiment	
n	$\alpha = 3°$ $\gamma = 45°$	$\alpha = 45°$ $\gamma = 3°$	$\alpha = 5°15'$ $\gamma = 35°$	$\alpha = 35°$ $\gamma = 5°15'$	$\alpha = 8°$ $\gamma = 45°$	$\alpha = 45°$ $\gamma = 8°$	α γ	γ α
−3	0.363	0.252	0.427	0.329	0.483	0.381	0.31	0.23
−2	0.198	0.051	0.204	0.031	0.370	0.109	0.39	0.06
−1	0.439	0.697	0.369	0.640	0.147	0.510	0.30	0.71

$\gamma = 45°$, $L/d = 60\%$) the predicted power is too small compared with experiment. For Ag, all the profiles give a peak at 3500 Å. Besides this peak, the experimental points generally lie close to the theoretical points for large profile variations. This explains why the previous average profile gives good results. Figure 18 shows the ratio of the power radiated by Ag to the power radiated by Al with the same profile. It is remarkable that the experimental curve shows the same general characteristics as the theoretical curve: a fall after 3500 Å and a tendency toward unity at 5780 Å (for large λ one approaches the case of infinite conductivity). One example shows how the peak is diminished on changing the direction of the grooves. This perhaps explains, aside from contamination, why the peak is not as intense as calculated: The photograph (Fig. 10) shows that sometimes the sense of the grooves is not very well defined. (b) Influence of the shape of the grooves on the radiating diagrams: Here also a flat top L/d of up to 20% little alters the results from the average profile taken in Figs. 11 and 14. On the other hand, in the previously used profiles the shape of the radiation patterns deviates rapidly from the experimental observations. However, at 5780 Å (Al) we note a sharp variation in the pattern when the direction of the grooves is inversed (diminution of the second order to the advantage of the first order). Table I shows that we find this behavior for all the profiles studied. This could explain the distinctness of this effect in spite of the fluctuations of the profile.

Finally, we see that the average profile assumed initially for Al, which approaches the ideal profile of the constructor, fits the best. It permits the reconstitution of the variations as a function of the groove direction and of the metal. This is somewhat surprising since in the real profile there are large defects, but it seems to prove that the average profile has a physical meaning. At the same time it is felt that the theory being tested is well confirmed.

VI. CONCLUSION

After discussing the influence of some experimental parameters we showed what conditions are important in obtaining the Smith-Purcell effect, i.e., the diffraction radiation of the electron field. Good agreement was found between the experimentally measured line breadth and the theoretical prediction. The increase in intensity due to radiative transformation of plasma surface waves (in Ag) was clearly observed. The comparison of the absolute theoretical and experimental power both for Al and Ag was somewhat limited by the poor quality of the grating. However we showed from the theoretical variations of the profile shape that the theory is correct and allows one to calculate the influence of the grating metal as described by its dielectric constant. In conclusion, within the experimental accuracy the theory was well verified.[20]

ACKNOWLEDGMENTS

The author wishes to thank L. Capella (Laboratoire de Physique Cristalline, St. Jérôme-Marseille) for the profile determinations and A. Fornier (Laboratoire d' Optique, St. Jérôme-Marseille) for discussions concerning this subject.

*Part of a Doctorat d'Etat thesis submitted under the Centre National de la Recherche Scientifique, Report No. A.O. 5566.

[1]S. J. Smith and E. M. Purcell, Phys. Rev. 92, 1069 (1953).

[2]S. J. Smith, thesis (Harvard University, 1953) (unpublished).

[3]J. A. Bradshaw, *Proceedings of the Symposium on Millimeter Waves* (Polytechnic, Brooklyn, N. Y., 1959), Vol. 8, p. 223.

[4]K. Ishiguro and T. Tako, Opt. Acta 8, 25 (1961).

[5]W. W. Salisbury, J. Opt. Soc. Am. 52, 1315 (1962); and private communication.

[6]W. W. Salisbury, J. Opt. Soc. Am. 60, 1279 (1970).

[7]J. P. Bachheimer and J. L. Bret, Compt. Rend. 266, 902 (1968).

[8]J. L. Bret and J. P. Bachheimer, Compt. Rend. B269, 285 (1969).

[9]J. P. Bachheimer, J. Phys. (Paris) 31, 665 (1970).

[10]G. Toraldo di Francia, Nuovo Cimento 16, 61 (1960).

[11]Here we cannot check the procedure by energy-conservation criteria as used in plane-wave problems. However the validity is shown by using the exact (but more difficult) method of the integral equation; we have found in Ref. 14 for the infinite-conductivity case that the numerical results agree well with the Rayleigh approximation when both methods give good convergence. Let us recall that for infinitely shallow grooves with Rayleigh's approximation one finds the same radiation pattern as with an electrostatic image theory (perfect conductor) which predicts a zero intensity at θ_0 ($=\sin^{-1}\beta$). But in practice we do not have infinitely shallow grooves, and in conse-

quence, the zero does not generally exist.

[12]In the non-ultra-relativistic case, when the Rayleigh approximation is valid.

[13]J. L. Bret, D. I. thesis (Grenoble, 1968) (unpublished).

[14]J. P. Bachheimer, thesis (Grenoble, 1971) (unpublished).

[15]J. C. Devos, Physica 20, 690 (1954).

[16]P. Bousquet, L. Capella, A. Fornier, and J. Gonella, Appl. Opt. 8, 1229 (1969).

[17]G. Hass and J. E. Waylonis, J. Opt. Soc. Am. 51, 719 (1961).

[18]A. J. Braudmeier and E. T. Arakawa, Z. Physik 239, 337 (1970).

[19]R. H. Huebner, E. T. Arakawa, R. A. Macrae, and R. N. Hamm, J. Opt. Soc. Am. 54, 1434 (1964); L. G. Schultz, *ibid.* 44, 357 (1954); L. G. Schultz and F. R. Tangherlini, *ibid.* 44, 362 (1954).

[20]It is perhaps of interest to develop this theory to find a quantitative theory of radiative-surface-plasmon decay from irregularities when electrons bombard a plane surface.

PHYSICAL REVIEW B VOLUME 6, NUMBER 8 15 OCTOBER 1972

Deviations from Matthiessen's Rule Due to Phonon Spectrum Changes

Robert J. Berry

Division of Physics, National Research Council of Canada, Ottawa, Ontario, Canada and Department of Physics, University of Ottawa, Ottawa, Ontario, Canada

(Received 20 April 1972)

The deviations from Matthiessen's rule which would be expected to result from changes in the phonon spectrum of a metal when chemical or physical defects are introduced, have been analyzed in greater detail within the framework of the Bloch-Grüneisen theory. This work was prompted by certain contradictory statements appearing in the literature, and has led to a clarification of the situation regarding possible changes in the characteristic temperature θ_R. In addition, a fresh assessment of the applicability of this model to more recent experimental results is presented.

INTRODUCTION

The electrical resistivity of metals containing dilute concentrations of chemical or physical defects is to a first approximation given by Mattheissen's rule[1] (MR), which is usually expressed in the form

$$\rho(T) = \rho_i^p(T) + \rho(0) \ , \tag{1}$$

where $\rho(T)$ and $\rho(0)$ are the measured resistivities of the alloy (or physically deformed metal) at temperatures T(K) and 0(K), respectively, and $\rho_i^p(T)$ is the phonon resistivity of the ideally pure host metal, as derived from measurements on a relatively pure specimen. In the most precise measurements, particularly those extending to temperatures below 100 K, small deviations from MR have been clearly observed in many cases.[2-22] These deviations $\Delta(T)$ are usually expressed in the form

$$\Delta(T) = \rho(T) - \rho_i^p(T) - \rho(0) \tag{2}$$

or as

$$\frac{d\Delta(T)}{dT} = \frac{d\rho(T)}{dT} - \frac{d\rho_i^p(T)}{dT} \ , \tag{3}$$

where the right-hand side of Eq. (3) is simply the change in slope produced by the addition of defects.

In a considerable number of investigations the observed deviations from MR have been attributed totally, or in part, to changes in the phonon spectrum of the pure metal produced by the defects. These include investigations on various alloys[2-6] as well as cold-worked,[7-10] quenched,[11] and irradiated[10,12] metals. In nearly all of these studies the change in the phonon resistivity, associated with the phonon spectrum change, has been characterized simply by a change in the characteristic temperature θ_R used in the Bloch-Grüneisen expression[23] for $\rho_i(T)$. This expression may be written as

$$\rho_i(T) = c\theta_R^{-2} TG(\theta_R/T) \ , \tag{4}$$

where $G(\theta_R/T)$ is a tabulated integral function[23] of (θ_R/T) and c is a constant for any particular metal. In this particular type of analysis the parameter θ_R is considered to change from θ_p for the pure metal to θ_a for the "impure" or alloyed metal, while $\rho_i(T)$ correspondingly changes from $\rho_i^p(T)$ to $\rho_i^a(T)$. Moreover, it is usually assumed that this is the only source of deviation from MR, and therefore $\Delta(T) = 0$ when the more appropriate value $\rho_i^a(T)$ is used in Eq. (2), i.e.,

$$\rho(T) = \rho_i^a(T) + \rho(0) \ . \tag{5}$$

Various investigators have predicted specific changes in θ_R to account for the apparent deviations